Supplementary Information

Design of S, N-codoped Co-Fe dual-atom sites for efficient alkaline oxygen reduction

Ning He,[a] Yuanmiao Sun,[b,c] Xiaoyang Chen,[a] Jiaqi Wang,[a] Guojin Liang,[c]* Funian Mo[a,d]*

[a] *School of Materials Science and Engineering, Harbin Institute of Technology, Shenzhen, 518055, Guangdong, China. Email: mofunian@hit.edu.cn*

[b] *School of Material Science and Engineering, Nanyang Technological University, 50 Nanyang Avenue, Singapore 639798, Singapore.*

[c] *Faculty of Materials Science and Engineering, Low Dimensional Energy Materials Research Center, Shenzhen Institutes of Advanced Technology, Chinese Academy of Sciences, 518055, Shenzhen, China. Email: gj.liang@siat.ac.cn*

[d] *School of Future Technology, Shenzhen Technology University, Shenzhen, 518055, Guangdong, China. Email: mofunian@sztu.edu.cn*

Experimental section

Synthesis of Co-Fe-SNC and Co-Fe-NC

To synthesize Co-Fe-SNC, Zn(NO3)$_2$·6H$_2$O (5.95 g) and cobalt (II) acetylacetonate (5.14 g) were added into methanol (200 ml), stirred and sonicated for 15 min. The resulting clear solution was labeled as solution A. In a separate container, 2-Methylimidazole was dissolved in methanol (200 ml), and the resulting clear, colorless solution was labeled as solution B. Solution A was slowly poured into vigorously stirred solution B, and the stirring was continued for 30 min. After standing for 20 h, the resulting turbid mixture was collected by centrifugation and washed three times with methanol. The resulting product was then dispersed in methanol (200 ml). FeCl$_2$·4H$_2$O (3.98 g), 1,10-phenanthroline (72.1 g) and thiourea (761.2 mg) were dissolved in methanol (200 ml), and the resulting dark red solution was recorded as solution C. Solution C was poured into the methanol in which the product was dispersed, sonicated for 30 min and then stirred for 20 h. The reloaded product was collected by centrifugation and washed three times with methanol. After vacuum drying at 60 °C overnight, the product was calcined in an argon atmosphere at 900 °C for 3 hours, and the obtained black powder was Co-Fe-SNC. The synthesis of Co-Fe-NC is similar to that of Co-Fe-SNC, except that thiourea is not added.

Synthesis of Co-NC, Fe-NC and NC

The synthesis process for Co-NC follows the same procedure as the first half of Co-Fe-SNC. The mixture of solution A and solution B was stirred and left to stand before being collected through centrifugation. The obtained product was then calcined in an argon atmosphere at 900 °C for 3 hours, resulting in black powder identified was Co-NC. The synthesis process for Fe-NC was similar to that of Co-NC, with the exception of using FeCl$_2$·4H$_2$O (3.98 g) instead of cobalt (II) acetylacetonate (5.14 g). The synthesis process of NC is similar to that of Co-NC and Fe-NC, except that Fe or Co metal salts are not used.

Materials Characterization

Scanning electron microscopy (SEM) images were taken on a TESCAN MIRA LMS operated at 3 kV. HAADF-STEM images and Energy-dispersive X-ray spectroscopy (EDS) mappings were taken on an JEOL JEM-2100F operated at 200 keV. Atomic-resolution HAADF-STEM images were taken on a Titan Cubed Themis G2 300 operated at 300 keV. X-ray diffraction (XRD) patterns were collected using on a Rigaku/SmartLab at a scan rate of $5° \min^{-1}$ in the 2θ range of 10°-80°. X-ray photoelectron spectroscopy (XPS) tests were carried out on a Thermo Scientific K-Alpha with Al Kα radiation (hν = 1486.6 eV). Metal contents of the samples were analyzed by ICP-OES (Aglient 5110). The XAFS spectrum was tested at the Beijing synchrotron radiation source. The XANES and EXAFS data were processed with the ATHENA and ARTEMIS software packages.

Electrochemical Measurements

To prepare the catalyst ink, 4 mg of catalyst was uniformly dispersed in 960 μl isopropanol and 40 μl 5 wt% Nafion solution. ORR measurements were performed in a three-electrode system (CHI760E, CH Instruments), in which the Pt foil was the counter electrode and the Ag/AgCl electrode (saturated KCl) was the reference electrode. The working electrode was assembled by utilizing a catalyst ink on a glassy carbon electrode (GCE) with a diameter of 5 mm. Before testing, a 5 μL drop of the ink was applied onto the GCE to form a uniform catalyst layer. ORR activity was recorded in 0.1 M KOH solution at room temperature (~25 °C) with 1,600 rpm at 10 mV s^{-1}. The net current density polarization curves were obtained by subtracting the corresponding LSV curve at nitrogen saturation from the LSV curve at oxygen saturation to exclude the effect of capacitance on ORR activity. Gas-saturated 0.1M KOH solutions were achieved by purging the electrolyte with a specific gas for at least 30 minutes. All potentials measured were calibrated to the reversible hydrogen electrode using the following equation: $E_{(RHE)} = E_{(Ag/AgCl)} + 0.197 + 0.059 * pH$.

Zinc-air battery performance tests

The zinc–air battery is composed of catalyst-coated carbon cloth as the air cathode, a Zn plate (0.1 mm in thickness) as the anode, and a 6 M KOH + 0.2 M $Zn(Ac)_2$ aqueous solution as the electrolyte. The air electrode was fabricated by spreading the as-prepared catalyst ink onto carbon cloth at a loading of 1 mg cm^{-2}. All measurements of zinc-air batteries were performed in ambient environment at room temperature. The specific capacity of zinc-air batteries was calculated based on the difference in quality of zinc plates before and after long-term discharging process. The discharge polarization curves were obtained using a CHI760E electrochemical workstation with a scan rate of 10 mV s^{-1}.

Computational methods

The density functional theory (DFT) calculations were performed using Vienna Ab Initio Simulation Package (VASP) equipped with the plane-wave basis sets and the projector augmented-wave method.[1, 2] The electron exchange and correlation energy were handled by a Perdew-Burke-Ernzerhof (PBE) parametrized generalized gradient approximation.[3, 4] The energy cutoff was defined as 500 eV. k-space integration was sampled using a $3 \times 3 \times 1$ Monkhorst–Pack grid. The convergence criteria for energy and force were set to 10^{-6} eV and 0.02 eV $Å^{-1}$, respectively. A vacuum slab of 15 Å was inserted in the z direction for surface isolation to avoid the mutual effect between neighboring images. The adsorption energy was calculated according to the following equation: $E_{ads} = E_{(slab+adsorbate)} - E_{slab} - E_{adsorbate}$, where $E_{(slab+adsorbate)}$ is the energy of the specie adsorbed on the surface, E_{slab} is the energy of the bare surface and $E_{adsorbate}$ is the energy of the gas-phase molecule.[5, 6]

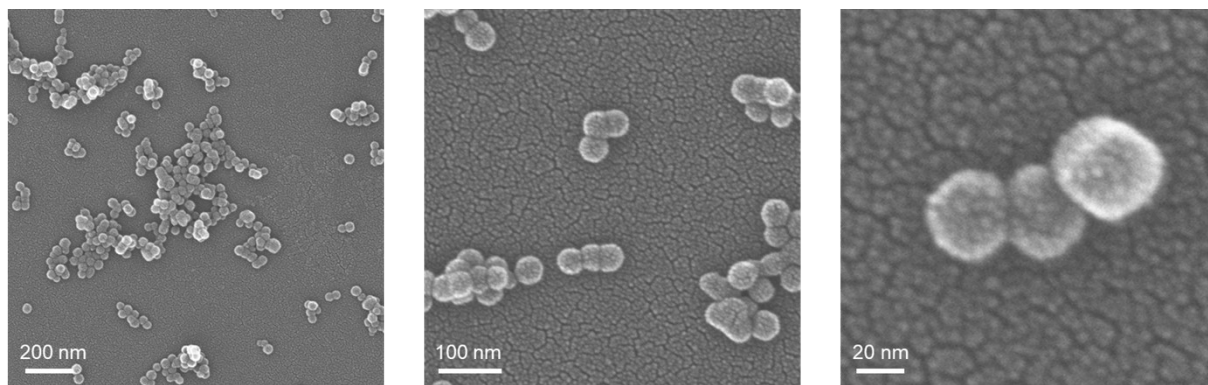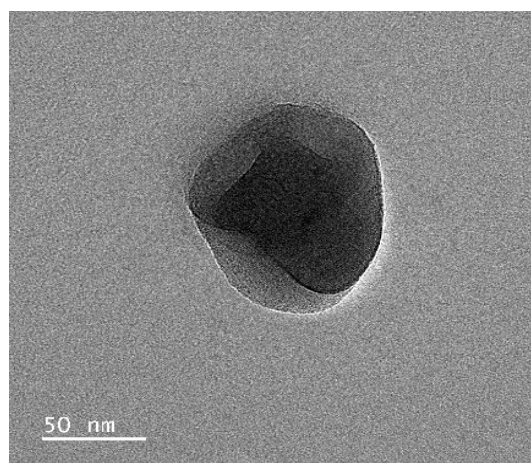**Figure S1.** SEM images of Co-Fe-SNC at different magnifications.
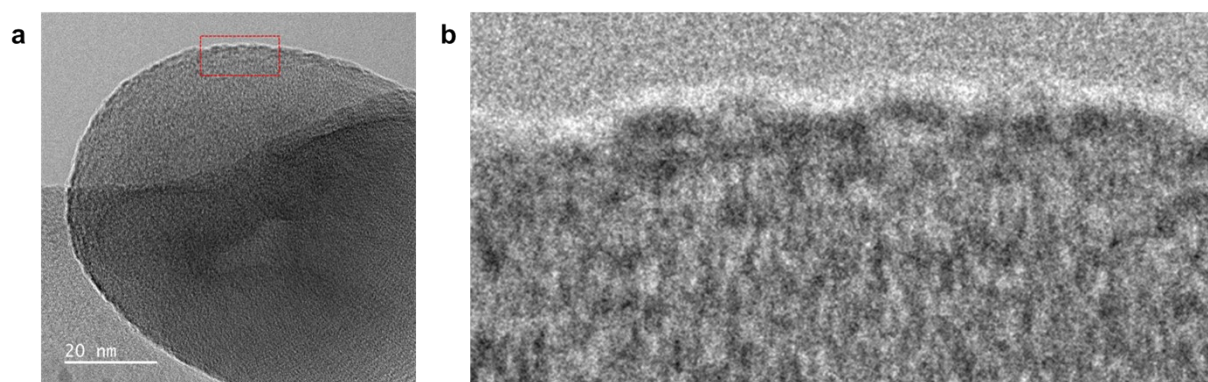

Figure S2. A TEM image of Co-Fe-SNC.

Figure S3. HRTEM image (**a**) of Co-Fe-SNC and the enlarged image (**b**) corresponding to the red box.
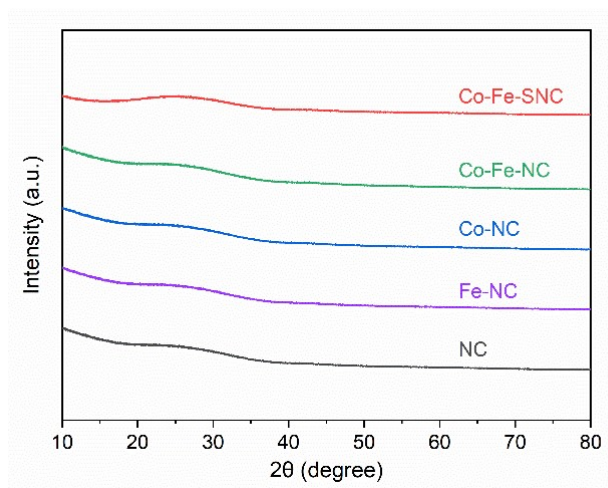
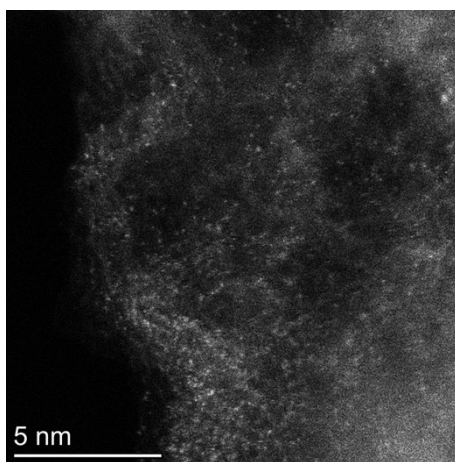**Figure S4.** XRD patterns of Co-Fe-SNC, Co-Fe-NC, Co-NC, Fe-NC and NC.

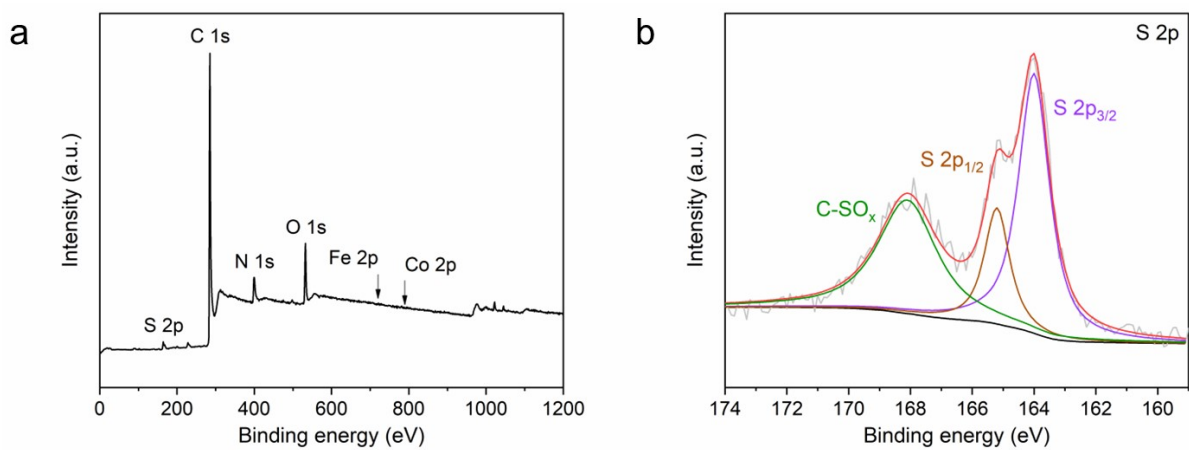
Figure S5. Aberration-corrected HAADF-STEM image of Co-Fe-SNC.

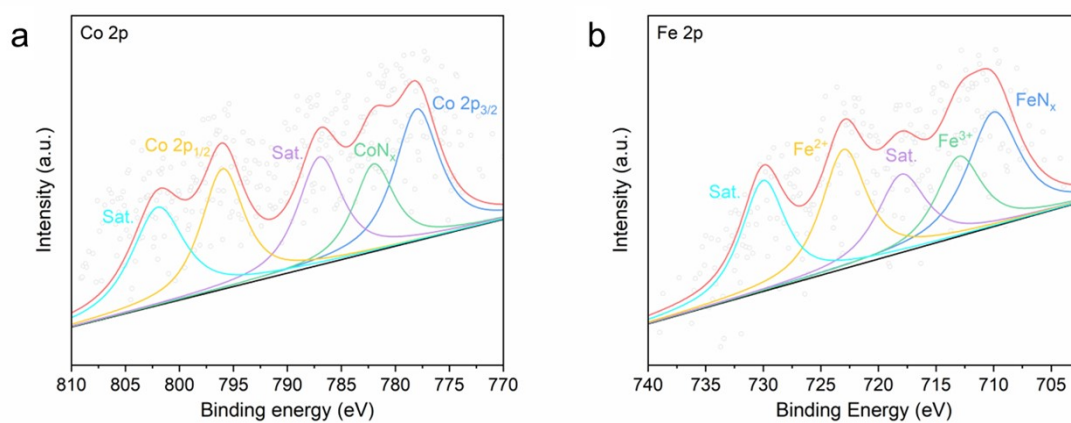**Figure S6.** XPS survey spectrum of Co-Fe-SNC catalyst (**a**) and corresponding high-resolution of S 2p (**b**).

Figure S7. High-resolution XPS Co 2p (**a**) and Fe 2p (**b**) spectra of Co-Fe-SNC.
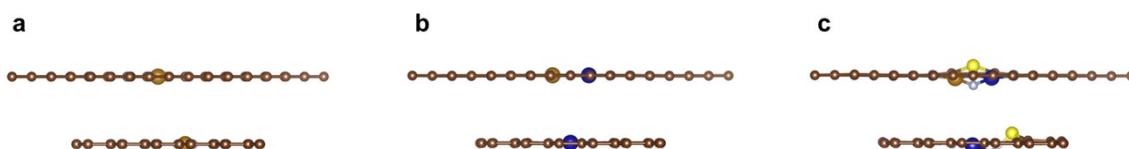

Figure S8. Front and side views of the optimal geometric models for Fe-NC (**a**), Co-Fe-NC (**b**), and Co-Fe-SNC (**c**).

Table S1. The proportion of different nitrogen species for the catalysts from XPS results.

Sample	Pyridinic N (%)	Pyrrolic N (%)	Graphitic N (%)	Oxidized N (%)	M-N (%)
Co-Fe-SNC	24.2	15.4	38.4	11.9	10.1
Co-Fe-NC	37.1	12.4	25.8	5.9	18.8
Co-NC	30.6	10.5	29.8	11.3	17.8
Fe-NC	27.3	13.6	33.9	8.9	16.3
NC	49.4	21.1	18.8	10.6	NA

Table S2. Structural parameters extracted from the Co K-edge EXAFS fitting.

Sample	Path	N	R (Å)	σ^2 (10^{-3} Å^2)	R factor (%)
Co-Fe-SNC	Co-N	4.0	1.94 ± 0.01	7.6 ± 2.3	0.43
	Co-Fe	1.0	2.33 ± 0.02	4.3 ± 2.3	

*N is the coordination number; R is interatomic distance (the bond length between central atoms and surrounding\coordination atoms); σ^2 is Debye-Waller factor (a measure of thermal and static disorder in absorber-scatterer distances); R factor is used to value the goodness of the fitting.

Supplementary References

1. G. Kresse and J. Furthmüller, *PHYS. REV. B*, 1996, **54**, 11169–11186.

2. G. Kresse and J. Hafner, *PHYS. REV. B*, 1993, **47**, 558-561.

3. G. Kresse and J. D., *PHYS. REV. B*, 1999, **59**, 1758-1775.

4. J. P. Perdew, K. Burke and M. Ernzerhof, *PHYS. REV. LETT.*, 1996, **77**, 3865–3868.

5. Y. Chen, S. Ji, S. Zhao, W. Chen, J. Dong, W. C. Cheong, R. Shen, X. Wen, L. Zheng, A. I. Rykov, S. Cai, H. Tang, Z. Zhuang, C. Chen, Q. Peng, D. Wang and Y. Li, *Nat. Commun.*, 2018, **9**, 5422.

6. K. Song, Y. Feng, X. Zhou, T. Qin, X. Zou, Y. Qi, Z. Chen, J. Rao, Z. Wang, N. Yue, X. Ge, W. Zhang and W. Zheng, *Appl. Catal., B*, 2022, **316**, 121591.